





Intercellular Communication as a Series of Narrow Escape Problems

Aoife Hughes , Christine Faulkner , Richard J. Morris , and Melissa Tomkins 

Abstract—Molecular communication is key for multicellular organisms. In plants, the exchange of nutrients and signals between cells is facilitated by tunnels called plasmodesmata. Such transport processes in complex geometries can be simulated using particle-based approaches, these, however, are computationally expensive. Here, we evaluate the narrow escape problem as a framework for describing intercellular transport. We introduce a volumetric adjustment factor for estimating escape times from non-spherical geometries. We validate this approximation against full 3D stochastic simulations and provide results for a range of cell sizes and diffusivities. We discuss how this approach can be extended using recent results on multiple trap problems to account for different plasmodesmata distributions with varying apertures.

Index Terms—Narrow escape problem, diffusion, signalling, intercellular communication, plasmodesmata, symplastic transport.

I. INTRODUCTION

DEFINING features of higher organisms include multicellularity, cell differentiation and tissue specificity, all of which rely on communication and coordination between cells [1]. Cells can communicate to one another using mechanical, electrical and chemical signals [2]. Whilst plants employ multiple instantiations of all these signalling strategies to launch appropriate responses to changes in their environment and to coordinate growth, many key processes are governed by the exchange of chemical species (ions, hormones, peptides, short RNA, and macromolecules such as proteins and mRNA [3]), thus placing molecular communication [4]–[7] at the core of plant development.

Plant cells are connected by channels called plasmodesmata that link the cytoplasm from neighboring cells to form the symplast [8], creating a prime route for signalling molecules (Fig. 1 A). The flux of signalling molecules can

Manuscript received July 3, 2020; revised January 20, 2021; accepted May 10, 2021. Date of publication May 26, 2021; date of current version June 29, 2021. This work was supported in part by EU Horizon 2020 ERC “Intercellar;” in part by EU Horizon 2020 ERC “Plamorf;” in part by the Biotechnology and Biological Sciences Research Council (BBSRC) DTP; and in part by BBSRC Institute Strategic Programme “Plant Health” under Grant BB/P012574/1. The associate editor coordinating the review of this article and approving it for publication was J. Hyttinen. (Corresponding author: Melissa Tomkins.)

Aoife Hughes, Richard J. Morris, and Melissa Tomkins are with the Department of Computational and Systems Biology, John Innes Centre, Norwich NR4 7UH, U.K. (e-mail: aoife.hughes@jic.ac.uk; richard.morris@jic.ac.uk; melissa.tomkins@jic.ac.uk).

Christine Faulkner is with the Department of Crop Genetics, John Innes Centre, Norwich NR4 7UH, U.K. (e-mail: christine.faulkner@jic.ac.uk)

Digital Object Identifier 10.1109/TMBC.2021.3083719

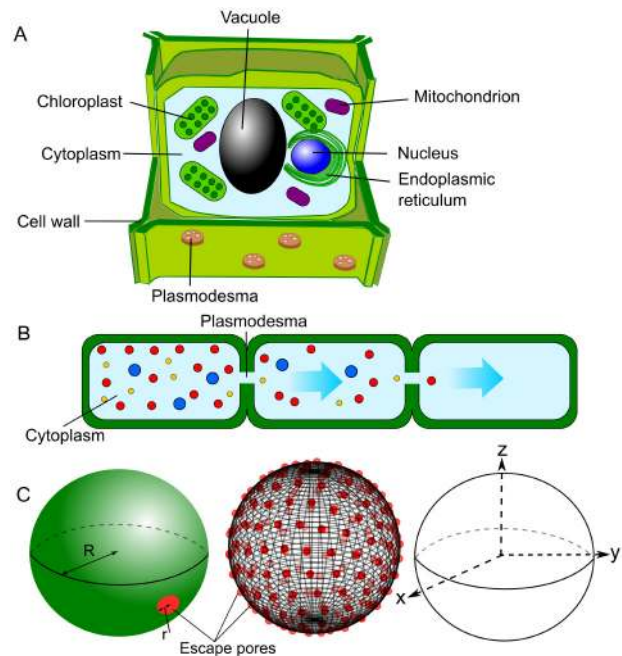


Fig. 1. Cell-to-cell molecular communication can be viewed as a series of narrow escape problems. (A) Plant cells are complex systems that are surrounded by cell walls. Plasmodesmata allow for the movement of molecules between cells. Individual cells can be idealised as a volume of reflecting (plasma membrane) and non-reflecting (plasmodesmata) regions (B). Narrow escape solutions are calculated for radii of a sphere and escape pore(s), denoted as R and r respectively. Solutions are provided for both a single escape and multiple, uniformly distributed escape pores (C).

be influenced by changes to plasmodesmatal density and importantly by adjusting plasmodesmatal aperture in response to many internal and external cues [9]. A wide range of processes have been shown to depend on symplastic communication [10]. An important problem in plant biology is, therefore, to understand how molecular communication is regulated by plasmodesmata.

The symplastic mediated transfer of molecules between cells is largely determined by size and density of plasmodesmata and the diffusivity of the molecules. The aperture of individual plasmodesmata may be altered by the deposition or removal of callose in the cell wall [11]. This process changes the size and number of particles that may be transported, often described by the size exclusion limit [8]. Methods for quantifying the parameters of plasmodesmata density, size and aperture are costly and experimentally labour-intensive. As a result in recent years there has been an increased interest

in the modelling of intercellular transport [12]–[14]. Despite metabolically active plant cells typically undergoing cytoplasmic streaming and the fact that the cytoplasm is a highly crowded environment that is far from the conditions of a dilute solution, movement of several chemical species within cells has been shown to be captured well by a diffusion model. Models of cell-to-cell movement use diffusion within each cell coupled with flux through the wall as a function of concentration differences on either side of the plasmodesmata. The behavior of such models can be summarised using an *effective diffusivity* for cell-to-cell transport that takes cell wall permeabilities into account.

Our approach builds on recent results from statistical mechanics to describe molecular communication between neighboring cells. An occurring task of statistical physics is to evaluate how long a diffusing particle will take to find a defined position on the boundary of an otherwise reflecting surface. This is known as the narrow escape problem for which analytical solutions have been derived for simple geometries in two and three dimensions [15]–[17]. This approach has previously been applied by others to problems in biology and chemistry that involve microdomains, such as calcium dynamics in dendritic spines, chemical reactions, and vesicle trafficking [15], [17]. For an overview of related problems the reader is referred to these excellent reviews [17], [18].

For a three-dimensional sphere of volume V with a non-reflecting area of radius r , the mean narrow escape time, τ , is given by

$$\tau = \frac{V}{4rD}, \quad (1)$$

where D is the diffusion constant of the particle within the volume [15]. These results have recently been extended to cases with more than one escape region [16]. For a three-dimensional unit sphere with N uniformly distributed escape regions of equal radius, r_{pd} , the mean narrow escape time can be approximated by

$$\tau = \frac{f(r_{pd})}{3D\kappa(r_{pd})} + \frac{1}{15D}, \quad (2)$$

for $N \gg 1$ and $r_{pd} \ll 1$, in which the functions $f(r_{pd})$ and $\kappa(r_{pd})$ have been defined as

$$f(r_{pd}) = r - \frac{r_{pd}^2}{\pi} \log r_{pd} + \frac{r_{pd}^2}{\pi} \log 2 \quad (3)$$

$$\kappa(r_{pd}) = \frac{Nr_{pd}^2}{\pi - 2r_{pd}\sqrt{N}}. \quad (4)$$

Note that for Eqs. (3)-(4), quantities that include length-scales (such as radii, areas, volumes, diffusion constants) must be scaled accordingly for problems with spheres of radii different from one.

Such equations have the advantage of being simple and fast, yet the extension to more complex geometries is still under development. Here, we investigate how equations based on the spherical geometry shown in Fig. 1 C can be used to describe the molecular communication between plant cells. We first compare full 3D stochastic simulations of diffusion [19] to the

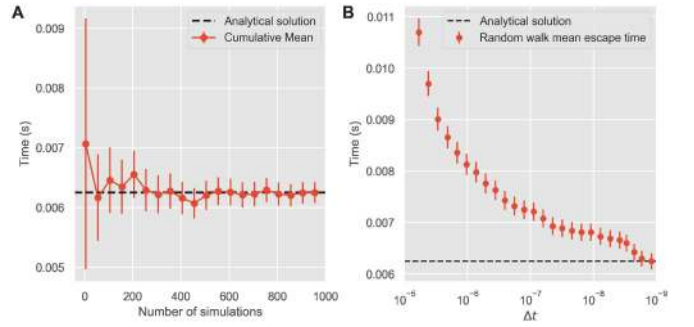


Fig. 2. The analytical approximation of the mean narrow escape time captures the behavior computed from random walk simulations. $V = 1 \mu\text{m}^3$, $r = 0.1 \mu\text{m}^2$, $D = 400 \mu\text{m}^2/\text{s}$ results in $\tau = 0.00625$ s, standard error is given for simulations. (A) The cumulative mean of the escape time converges after about 500 simulations. (B) The evaluation of different Δt values shows a good agreement between the simulation and the analytical solution for $\Delta t \leq 1.0 \times 10^{-9}$ s.

mean narrow escape time equation for a single escape region on a sphere, Eq. (1), and then explore deviations from a sphere. We introduce a *volumetric adjustment factor* to approximate the mean narrow escape time for shapes more representative of plant cells. Finally, we explore how changing the density of plasmodesmata, under the constraint of total plasmodesmata area remaining constant, influences the estimation of the mean narrow escape time. We briefly outline ongoing work and future directions.

II. RESULTS

A. Analytical Approximations for the Mean Narrow Escape Time Agree With Estimates From Large-Scale Random Walk Simulations

We first set up random walk simulations in order to compare to the equation for the mean narrow escape time. For random walk simulations, the step size, Δx , needs to be carefully matched to the time step and the diffusion constant, D , following [20] we used $\langle \Delta x \rangle^2 = 6D\Delta t$. Small time steps lead to more accurate results at the cost of longer simulation times. We monitored the convergence as a function of Δt and based on our results, we chose $\Delta t = 10^{-9}$ s for all subsequent simulations. As expected, for a particle diffusing in a sphere with a single exit, averaging the escape time over an increasing number of simulations converges towards the analytical approximation (Figs. 2 A–B).

B. An Effective Diffusion Constant Can Be Used to Summarise the Behavior Predicted by the Narrow Escape Solutions

Plasmodesmata allow for the flux of molecules between cells through cell walls. The distribution and geometry of plasmodesmata can be described by the cell wall permeability, which can result in a significant change to the movement of the molecule. For the 1D case this change in movement can be captured by an *effective diffusion constant* D_{eff} ,

$$D_{\text{eff}} = \frac{Dql}{D + ql}, \quad (5)$$

TABLE I
PARAMETERS USED IN NARROW ESCAPE SIMULATIONS
AND EFFECTIVE DIFFUSION CALCULATIONS

Parameter	Value	Comment
R	$20 \mu\text{m}$	Cell radius
A	$5,026 \mu\text{m}^2$	Cell surface area, $4\pi R^2$
V	$33,510 \mu\text{m}^3$	Cell volume, $4\pi R^3/3$
D	$220 \mu\text{m}^2/\text{s}$	Diffusion constant [13]
q	$5 \mu\text{m}/\text{s}$	Cell wall permeability [13]
D_{eff}	$104.76 \mu\text{m}^2/\text{s}$	Effective diffusion constant, $2RDq/(D + 2Rq)$
r_{pd}	$0.025 \mu\text{m}$	Radius of plasmodesmatal opening [13]
n	$0.4 \mu\text{m}^{-2}$	Plasmodesmata density [13]
N	2010	Number of plasmodesmata per cell, nA
a	$3.95 \mu\text{m}^2$	Total escape area, $\pi r_{\text{pd}}^2 N$
r	$1.12 \mu\text{m}$	Total escape radius, $r_{\text{pd}}\sqrt{N}$

in which q the permeability of the cell wall and l the cell length [12]–[14].

We were interested in comparing the time to diffuse a given distance with the mean narrow escape time and to estimate an effective diffusion constant that captures the flux between cells. In the following, we ignore organelles and assume the full plant cell volume is available for diffusion. For a plant cell of radius $20 \mu\text{m}$, a molecule with a diffusion constant of $220 \mu\text{m}^2/\text{s}$ would take approximately $t = R^2/(6D) \approx 0.3 \text{ s}$ to diffuse from the centre to the cell wall. For comparison, the mean narrow escape time with only one exit (all parameters are listed in Table I), Eq. (1), leads to $\tau_1 \approx 33 \text{ s}$. A multi-escape geometry with N exits, Eq. (2), with the same total exit area results in mean narrow escape time of $\tau_N \approx 0.85 \text{ s}$. Using the mean narrow escape time, τ , and assuming the process can still be described by diffusion, we can compute an effective diffusion constant from $D_{\tau,\text{eff}} = R^2/(6\tau)$. Using the value of $\tau_N = 0.85 \text{ s}$ results in an effective diffusion constant of $D_{\tau,\text{eff}} = 78.43 \mu\text{m}^2/\text{s}$. Using the 1D approximation and the values in Table I results in $D_{\text{eff}} = 104.76 \mu\text{m}^2/\text{s}$ and a time of $\approx 0.64 \text{ s}$ to diffuse through the cell and then through the cell wall. Equating $D_{\tau,\text{eff}}$ with D_{eff} thus allows us to compute the cell wall permeability, q , for a cell with N plasmodesmata, each with a defined aperture.

Changes to plasmodesmata apertures in response to environmental cues can significantly impact intercellular flux [21]. Using Eq. (2), we evaluated a realistic range of plasmodesmata densities and apertures [13] and find that the mean narrow escape time is within the range of 0.73 to 1.36 s for a cell of length $40 \mu\text{m}$ under non-stressed conditions (Fig. 3). This time range is likely to increase significantly as plasmodesmata open or close further in response to environmental stress. Obtaining direct measurements of plasmodesmata geometry is experimentally challenging, however, measuring the flux between cells under different conditions would allow us to infer such changes in plasmodesmatal aperture by fitting the equations to experimental observations.

C. An Adjusted Cell Volume Can Be Used to Accurately Reproduce the Mean Narrow Escape Time for Complex Geometries

The mean narrow escape time equations used above were derived for a sphere. Solutions for more complex shapes are generally non-trivial to find and in particular for typical plant

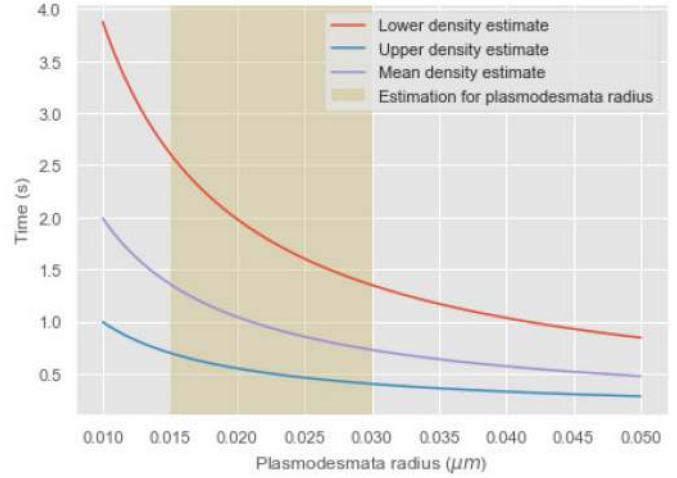


Fig. 3. Changes to plasmodesmata aperture impact on the mean narrow escape time. Plasmodesmata dynamically change their aperture to modulate cell-to-cell transport. The observed variation in radius of an individual plasmodesmata pore ranges between $0.015 \mu\text{m}$ and $0.03 \mu\text{m}$ (yellow shaded region). Estimates of the density of plasmodesmata vary between $0.2 \mu\text{m}^{-2}$ (red line) and $0.85 \mu\text{m}^{-2}$ (blue line), with a mean of $0.4 \mu\text{m}^{-2}$ (purple line).

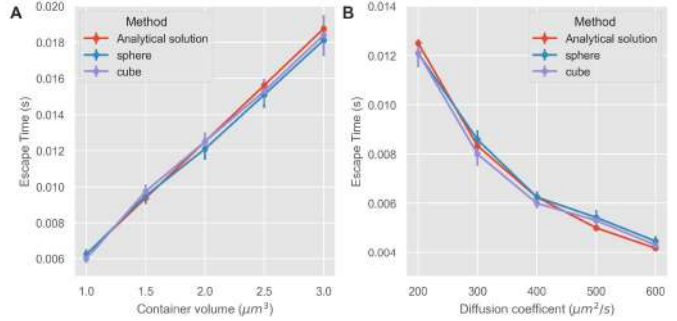


Fig. 4. Cell volume is a key determinant of the escape time. Simulation results from two different cell shapes (cube - purple, sphere - blue) as a function of volume V (A) and diffusion constant D (B) show a good fit with the analytical solution for a sphere of the same volume (red).

cell shapes analytical solutions are unlikely to exist. As a first step towards investigating deviations from a sphere, we performed random walk simulations with cubic domains. For this highly symmetric case, we find that cells of similar volume give rise to similar escape times (Fig. 4 A). As expected, this observation was consistent over different diffusion constants (Figs. 4 A–B). So for cubic cells, the mean narrow escape time solution for a sphere with the same volume as the cubic cell is a good approximation.

We next compared the narrow escape solutions with random walk simulations in spheroid domains with different degrees of elongation in the z -plane. All spheroids had a constant volume of $1 \mu\text{m}^3$, and the changes in their shape were quantified by the ratio of the surface areas of the smallest sphere to enclose the spheroid and the largest to fit within it (A_{outer} and A_{inner} , respectively). Unsurprisingly, we found that more extreme shapes deviate increasingly from the equation for the spherical case (Fig. 5 A). Thus, using the actual cell volume

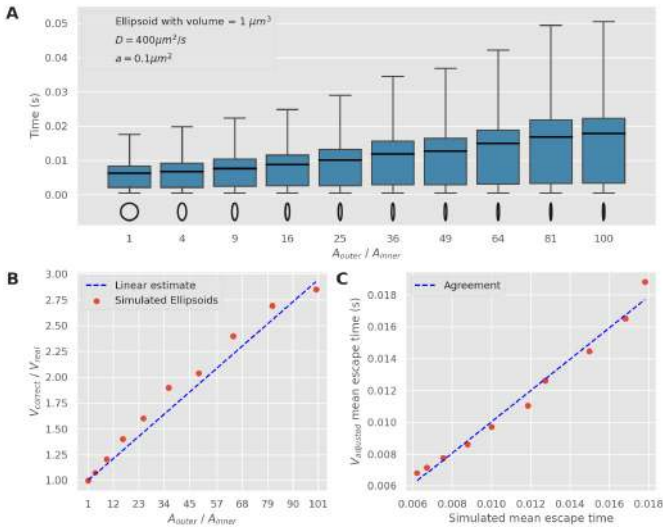


Fig. 5. Simulations show that mean narrow escape time estimates deviate as cells become less spherical (A). A volumetric correction factor for non-spherical shapes is derived by calculating the ratio of the volume that reproduces the mean narrow escape time (V_{correct}) to the real volume of the cell (V_{real}) as a function of the ratio of areas for the smallest containing sphere (A_{outer}) and the largest sphere which fits within the shape (A_{inner}) (B). Using this adjusted volume ($V_{\text{adjusted}} = g_V V_{\text{real}}$, where g_V is the volumetric correction factor from (B)) the analytical solutions agree well with simulated escape time estimates (C).

in the above narrow escape equations would lead to inaccurate escape time estimates the more the cell deviates from a sphere.

As any escape time can be viewed as arising from a sphere, we asked what the volume of that sphere would have to have been to reproduce the data we generated for different cell shapes. We denote the actual cell volume by V_{real} and the volume that gives the correct mean narrow escape time as V_{correct} . We describe the shape of each cell by the largest sphere we could fit within the cell and smallest sphere we could fit around the cell, which we characterise by the area ratio, $A_{\text{outer}}/A_{\text{inner}}$. Plotting the ratio of $V_{\text{correct}}/V_{\text{real}}$ over $A_{\text{outer}}/A_{\text{inner}}$, (Fig. 5 B), allows us to estimate a *volumetric adjustment factor* that when multiplied by the actual cell volume provides an accurate estimate of the mean narrow escape time for a spherical geometry. Escape time simulations for shapes not used in the derivation of the correction factor (Fig. 5 B) demonstrates we can achieve a good agreement between simulations and the mean narrow escape time equations using the adjusted volume (Fig. 5 C).

III. CONCLUSION

Molecular communication governs plant responses to the environment, growth and development. An understanding of the processes and parameters that determine these signaling events will therefore contribute to addressing important challenges in plant biology. There is currently little consensus regarding the most appropriate methods to represent inter-cellular communication networks in plants [12], [22]. In this contribution we explored the use of previously derived analytical solutions of the narrow escape problem as a potential method for modelling molecular communication in plants. As has previously been demonstrated [15], [16], [23], we found

an excellent agreement between 3D stochastic simulations and mean narrow escape equations for diffusing particles within a sphere. We then show how cell wall permeability and an effective diffusion constant can be computed from mean narrow escape solutions, allowing for the comparability with other approaches. Furthermore, we explore the impact of plasmadesmal densities and apertures on the molecular movement. To evaluate the potential of this approach for more realistic cell geometries, we explored different shapes. Unsurprisingly, this approximation becomes increasingly less accurate the more the shapes deviate from a sphere. Using a simple shape metric we empirically derived a volumetric adjustment factor that allows us to obtain accurate estimates of the mean narrow escape time for non-spherical cells. How well the equations can represent realistic plant cell shapes remains to be shown. However, from the analysis over multiple cell shapes we might expect that while each cell may be poorly described by a sphere, molecular movement over several cells within a tissue may on average still be well represented by such an approach if the volumes of the sphere are adjusted accordingly. As the volume is a key determinant of the mean narrow escape time, improving our estimates of the volume available for diffusion within a cell could be important (the cytoplasm is typically less than 10% of the total volume). Other key parameters include plasmodesmata density and aperture, both of which are regulated throughout development. Future work will investigate different plasmodesmata arrangements and aperture sizes on molecular transport for more realistic cell geometries and multiple cells. Inferring changes to either of these key plasmodesmata parameters (under the assumption that the other is known) for different perturbations to experimental conditions will shed light on the extent of plasmodesmata regulation and its impact of cell-to-cell communication.

REFERENCES

- [1] J. Tilsner, W. Nicolas, A. Rosado, and E. M. Bayer, "Staying tight: Plasmodesmal membrane contact sites and the control of cell-to-cell connectivity in plants," *Annu. Rev. Plant Biol.*, vol. 67, no. 1, pp. 337–364, 2016.
- [2] K. H. Edel, E. Marchadier, C. Brownlee, J. Kudla, and A. M. Hetherington, "The evolution of calcium-based signalling in plants," *Current Biol.*, vol. 27, no. 13, pp. R667–R679, Jul. 2017.
- [3] W.-G. Choi, G. Miller, I. Wallace, J. Harper, R. Mittler, and S. Gilroy, "Orchestrating rapid long-distance signaling in plants with Ca²⁺, ROS and electrical signals," *Plant J.*, vol. 90, no. 4, pp. 698–707, 2017.
- [4] T. Nakano, "Molecular communication: A 10 year retrospective," *IEEE Trans. Mol. Biol. Multi-Scale Commun.*, vol. 3, no. 2, pp. 71–78, Jun. 2017.
- [5] A. Ahmadzadeh, V. Jamali, and R. Schober, "Stochastic channel modeling for diffusive mobile molecular communication systems," *IEEE Trans. Commun.*, vol. 66, no. 12, pp. 6205–6220, Dec. 2018.
- [6] V. Jamali, A. Ahmadzadeh, W. Wicke, A. Noel, and R. Schober, "Channel modeling for diffusive molecular communication? A tutorial review," *Proc. IEEE*, vol. 107, no. 7, pp. 1256–1301, Jul. 2019.
- [7] A. Noel, K. C. Cheung, and R. Schober, "Bounds on distance estimation via diffusive molecular communication," in *Proc. IEEE Global Commun. Conf.*, 2014, pp. 2813–2819.
- [8] K.-J. Lu, F. R. Danila, Y. Cho, and C. Faulkner, "Peeking at a plant through the holes in the wall—Exploring the roles of plasmodesmata," *New Phytol.*, vol. 218, no. 4, pp. 1310–1314, 2018.
- [9] R. E. Sager and J.-Y. Lee, "Plasmodesmata at a glance," *J. Cell Sci.*, vol. 131, no. 11, Jun. 2018, Art. no. jcs209346.

- [10] J. D. Petit, Z. P. Li, W. J. Nicolas, M. S. Grison, and E. M. Bayer, "Dare to change, the dynamics behind plasmodesmata-mediated cell-to-cell communication," *Current Opin. Plant Biol.*, vol. 53, pp. 80–89, Feb. 2020.
- [11] N. De Storme and D. Geelen, "Callose homeostasis at plasmodesmata: Molecular regulators and developmental relevance," *Front. Plant Sci.*, vol. 5, p. 138, Apr. 2014.
- [12] E. E. Deinum, B. M. Mulder, and Y. Benitez-Alfonso, "From plasmodesma geometry to effective symplasmic permeability through biophysical modelling," *eLife*, vol. 8, Nov. 2019, p. e49000.
- [13] C. Gao *et al.*, "Directionality of plasmodesmata-mediated transport in Arabidopsis leaves supports auxin channeling," *Current Biol.*, vol. 30, no. 10, pp. 1970–1977, 2020.
- [14] H. L. Rutschow, T. I. Baskin, and E. M. Kramer, "Regulation of solute flux through plasmodesmata in the root meristem," *Plant Physiol.*, vol. 155, no. 4, pp. 1817–1826, 2011.
- [15] Z. Schuss, A. Singer, and D. Holcman, "The narrow escape problem for diffusion in cellular microdomains," *Proc. Nat. Acad. Sci.*, vol. 104, no. 41, pp. 16098–16103, Oct. 2007.
- [16] A. F. Cheviakov and D. Zawada, "Narrow-escape problem for the unit sphere: Homogenization limit, optimal arrangements of large numbers of traps, and the N2 conjecture," *Phys. Rev. E, Stat. Phys. Plasmas Fluids Relat. Interdiscip. Top.*, vol. 87, no. 4, 2013, Art. no. 042118.
- [17] D. Holcman and Z. Schuss, "The narrow escape problem," *SIAM Rev.*, vol. 56, no. 2, pp. 213–257, 2014. [Online]. Available: <https://doi.org/10.1137/120898395>
- [18] P. C. Bressloff and J. M. Newby, "Stochastic models of intracellular transport," *Rev. Mod. Phys.*, vol. 85, pp. 135–196, Jan. 2013. [Online]. Available: <https://link.aps.org/doi/10.1103/RevModPhys.85.135>
- [19] A. Hughes, R. J. Morris, and M. Tomkins, "PyEscape: A narrow escape problem simulator package for Python," *J. Open Source Softw.*, vol. 5, no. 47, p. 2072, 2020.
- [20] E. A. Codling, M. J. Plank, and S. Benhamou, "Random walk models in biology," *J. Royal Soc. Interface*, vol. 5, no. 25, pp. 813–834, 2008.
- [21] C. Faulkner *et al.*, "LYM2-dependent chitin perception limits molecular flux via plasmodesmata," *Proc. Nat. Acad. Sci.*, vol. 110, no. 22, pp. 9166–9170, 2013.
- [22] F. Cleri, "Agent-based model of multicellular tumor spheroid evolution including cell metabolism," *Eur. Phys. J. E*, vol. 42, no. 8, p. 112, Aug. 2019.
- [23] G. Oshanin, M. Tamm, and O. Vasilyev, "Narrow-escape times for diffusion in microdomains with a particle-surface affinity: Mean-field results," *J. Chem. Phys.*, vol. 132, no. 23, 2010, Art. no. 06B607.

Aoife Hughes received the B.Sc. degree in computer science from Aberystwyth University, Wales, U.K., in 2018. She is currently pursuing the Ph.D. degree in computational biology with John Innes Centre, Computational and Systems Biology, England, U.K. under the supervision of Prof. R. J. Morris. She has authored or coauthored more than five research papers in the field of plant biology. Her research interests include modeling of plasmodesmata facilitated communications.



Christine Faulkner received the B.Sc. (Hons.) and Ph.D. degrees from the University of Sydney, Australia, and held postdoctoral positions with the University of Edinburgh, the John Innes Centre, and the Sainsbury Laboratory, Norwich, that covered plasmodesmal biology and plant immunity. She started her independent research programme studying cell-to-cell communication during plant-microbe interactions with Oxford Brookes University and became a Group Leader with the John Innes Centre in 2013.



Richard J. Morris received the B.Sc. degree in physics and the M.Sc. degree in theoretical physics from the University of Graz, Austria, and the Ph.D. degree in computational biology from the University of Graz and the European Molecular Biology Laboratory (EMBL) in 2000. He held postdoctoral research positions with Global Phasing Ltd., and the European Bioinformatics Institute (EMBL-EBI). He then moved to a group leader position with the John Innes Centre in 2005. He was promoted to Head of the Department for Computational and Systems Biology in 2010, before taking on the role of an Associate Research Director and an Institute Strategic Programme Leader in 2013. His research aims to shed light on the physics of information processing in plants.



Melissa Tomkins received the Ph.D. degree in complex systems simulation from the National Oceanography Centre, University of Southampton, Southampton, in 2016. She is currently a Postdoctoral Researcher with Richard Morris' Lab, Department of Computational and Systems Biology, John Innes Centre, Norwich. Her research interests include individual-based and multilevel modeling, particularly how these methods can be used to understand communication in plants.